# 2025年臺灣國際科學展覽會 優勝作品專輯

作品編號 090016

參展科別 醫學與健康科學

作品名稱 Analyzing Glucose Metabolism Connectivity in Huntington's Disease Using Dynamic Glucose-Enhanced MRI in zQ175 and R6/2 KI Mouse Models

得獎獎項 一等獎

美國國際科技展覽會 ISEF

青少年科學獎

青少年科學獎

就讀學校 臺北市數位實驗高級中等學校

指導教師 陳育文

黄聖言

作者姓名 呂顥天

關鍵詞 <u>Dynamic Glucose-Enhanced Magnetic Resonance</u>

<u>Imaging (DGE MRI), Huntington Disease, Neural</u>

Connectivity

# 作者簡介



我是呂顥天,目前就讀於臺北市數位實驗高中二年級,對醫學影像、神經科學、資 料科學極感興趣,閒暇之餘熱愛研究數位治理政策與法規、攝影和作曲。

# 2025 年臺灣國際科學展覽會 研究報告

區別:

科別:醫學與健康科

作品名稱:Analyzing Glucose Metabolism Connectivity in Huntington's Disease Using Dynamic Glucose-Enhanced MRI in zQ175 and R6/2 KI Mouse Models

關鍵詞: Dynamic Glucose-Enhanced Magnetic Resonance Imaging (DGE MRI), Huntington Disease, Neural Connectivity

編號:

#### **ABSTRACT**

This study leverages DGE MRI to investigate glucose metabolism connectivity as a potential biomarker for Huntington's disease (HD) using two mouse models: zQ175 KI and R6/2 KI. Using Pearson correlation analysis, we calculated glucose connectivity between brain regions for both HD models and WT controls. Results revealed significant connectivity alterations in HD models, particularly in regions such as the thalamus, caudate putamen, and dentate gyrus, which are associated with HD-related pathophysiology.

To further examine metabolic patterns, we employed self-organizing maps (SOM) to cluster DGE MRI signal curves, identifying brain regions with similar glucose metabolism dynamics. The clustering analysis revealed discrete glucose metabolism zones, providing insights into spatial and temporal connectivity variations that might not be apparent in anatomical imaging alone. While clusters showed distinct temporal patterns—some with rapid initial signal increases, others with gradual changes—these metabolic shifts highlight SOM's utility in assessing brain region-specific metabolic behaviors.

The analysis indicates that glucose metabolism connectivity is notably disrupted in HD models, aligning with known HD pathology and reflecting both rapid and gradual disease progression observed in R6/2 and zQ175 KI mice, respectively. These findings underscore DGE MRI's potential as a novel imaging biomarker, offering insights into the metabolic disruptions in HD that may inform early diagnosis and therapeutic interventions. However, limitations in signal strength and the complexity of SOM clustering warrant further methodological refinements to enhance biomarker reliability.

In conclusion, our study supports the use of DGE MRI in identifying glucose metabolism connectivity disruptions as a viable HD biomarker, providing a robust framework for future studies targeting metabolic dysregulation in neurodegenerative diseases.

### 中文摘要

亨丁頓舞蹈症為與認知功能障礙密切相關的神經退行性疾病。本研究首次應用動態 葡萄糖強化磁振造影(DGE MRI)以了解葡萄糖代謝作為亨丁頓舞蹈症神經影像生物標 記的可行性,以分析大腦中不同區域之間的代謝關係。

本研究對腦區間葡萄糖代謝關聯性進行分析,並針對訊號進行自動化分群,觀察特定訊號樣態之特徵。於 zQ175 KI和 R6/2 KI小鼠中不同的連接性變化模式中,發現紋狀體和齒狀回之間葡萄糖代謝連接性具顯著變化,與已知病理一致,顯示 DGE MRI 作為臨床生物標記之潛力,以利及時診斷和監測該疾病。

這項開創性的研究探索了使用 DGE MRI 作為亨丁頓舞蹈症影像標記可行性,並詳細分析腦區間葡萄糖代謝相關性,不僅進一步對該疾病之病理更加深入了解,同時提高早期診斷、疾病監測和精準醫療應用發展,說明可能有針對代謝紊亂的潛在治療策略。

# TABLE OF CONTENT

ABSTRACT	I
中文摘要	II
I. INTRODUCTION	1
II. RELATED WORKS	4
A. FC Analysis Using rs-fMRI	4
B. FC of Huntington's Disease on Mice	4
C. DGE MRI FOR GLUCOSE METABOLISM CONNECTIVITY	6
III. MATERIALS AND METHODS	7
A. Animals	7
B. IMAGING ACQUISITION	7
C. Data Preprocessing	8
1) Data Conversion	8
2) Spatial Normalization	9
3) Label Co-registration	10
D. CONNECTIVITY ANALYSIS OF GLUCOSE METABOLISM	11
E. STATISTICAL ANALYSIS	11
F. CURVE CLUSTERING ANALYSIS	12
IV. RESULTS	13
A. zQ175 KI MICE	13
B. R6/2 KI MICE	15
C. CURVE CLUSTERING ANALYSIS	17
V. DISCUSSION	20
VI. CONCLUSION	23
VII REFERENCES	24

#### I. INTRODUCTION

Huntington's disease (HD), also known as Huntington's chorea, is a hereditary neurodegenerative disorder marked by progressive motor dysfunction, cognitive decline, and psychiatric disturbances (1). This autosomal dominant condition results from a mutation in the *HTT* gene, leading to an abnormal expansion of the CAG trinucleotide repeat within the gene (1, 2). The primary feature of HD is the gradual deterioration of voluntary motor control, manifesting in choreiform movements and eventually culminating in severe disability. Cognitive impairments include deficits in executive function, memory disturbances, and emotional dysregulation, which significantly affect the patient's quality of life. In addition, psychiatric symptoms, such as depression and psychosis, further exacerbate the burden of the disease. HD typically presents in mid-adulthood and progresses relentlessly, resulting in significant debilitation and a reduced life expectancy. Despite its devastating nature, ongoing research into the molecular mechanisms of HD holds promise for therapeutic interventions that may mitigate its clinical manifestations (3).

Recent studies have identified impairments in glucose metabolism in rat striatum cells (4), integrating metabolic and transcriptomic expression data from rodent models of HD. Beyond animal models, metabolic alterations have also been observed in the caudate nuclei of adult HD patients (5). These findings underscore the significance of investigating the relationship between neurodegenerative disorders and glucose metabolism, with the potential for glucose metabolism to serve as a clinical biomarker.

Under most conditions, glucose is considered the primary metabolic fuel of the brain, which enters the brain by facilitated diffusion across the blood-brain barrier, where its transport may adapt during changes in cerebral glucose metabolism, neural activation and changes in plasma glucose levels. As glucose metabolism connects with multiple other metabolic pathways, it generate adequate energy for neuronal cells to carry out their functions (6).

Traditionally, glucose concentration and metabolic rates have been measured using magnetic resonance (MR) spectroscopy (7, 8), which is known for its relatively slow speed and low resolution. However, recent advancements have been made in monitoring glucose levels in the brain and various organs using Magnetic Resonance Imaging (MRI) techniques such as Chemical Exchange Saturation Transfer (CEST) MRI (9-11). CEST MRI involves the application of radiofrequency (RF) irradiation to selectively saturate exchangeable protons found in low-concentration solutes, which are typically only detectable through Magnetic Resonance Spectroscopy (MRS). The saturated protons then transfer their saturation to water protons through proton exchange, which is subsequently replaced by non-saturated protons in a repeating cycle. This process enables CEST MRI to enhance signals from low-concentration metabolites, making them detectable alongside the more abundant bulk water protons. A specific configuration of CEST MRI, referred to as glucoCEST MRI, targets the hydroxyl protons in D-glucose. This method has demonstrated the ability to detect the presence of Dglucose or its derivatives in live subjects using MRI signals. Additionally, real-time changes in glucoCEST MRI signals following a bolus intravenous infusion of glucose, known as Dynamic Glucose-Enhanced (DGE) MRI, allow for the evaluation of alterations in glucose concentration within biological tissues. This technique provides valuable insights into glucose delivery, transport, and metabolic kinetics.

Resting-state functional MRI (rs-fMRI), first introduced by Biswal et al. in 1995, is a neuroimaging technique that elucidates intrinsic brain connectivity patterns by measuring spontaneous fluctuations in blood oxygenation level-dependent (BOLD) signals in subjects at rest, without the involvement of explicit cognitive tasks. rs-fMRI has been extensively applied in functional connectivity (FC) analysis of the brain, where correlations between time-series data from different brain regions allow medical experts to gain a deeper understanding of the pathophysiology of neurological diseases (12). Although both DGE MRI and rs-fMRI provide temporal information about brain activity, their temporal resolutions and clinical implications

differ significantly. Besides, the correspondence between cerebral glucose metabolism (indexing energy utilization) and synchronous fluctuations in blood oxygenation (indexing neuronal activity) is relevant for neuronal specialization and is affected by brain disorders, which shows the importance to research on cerebral glucose metabolism and its connectivity (13).

Despite the promise of DGE MRI in assessing glucose metabolism, connectivity analysis using this method has not yet been explored. Therefore, this study aims to investigate the brain connectivity of glucose metabolism in the brains of C57BL/6J mice with HD, specifically in the zQ175 KI and R6/2 KI models, to evaluate the potential of DGE MRI as a clinical biomarker through its connectivity features.

#### II. RELATED WORKS

#### A. FC Analysis Using rs-fMRI

rs-fMRI was first introduced in 1995, has demonstrated significant potential in identifying sensitive biomarkers for neurological diseases by detecting atypical FC within various resting-state networks (RSNs). This method has been applied to a broad range of neurological and psychiatric conditions, including schizophrenia (14-19), migraine (20-22), Alzheimer's disease (AD) (23-26), and depression (27-30). These disorders predominantly affect cognitive and mental functions, where detecting structural abnormalities has proven more challenging than identifying dysfunctions in cognitive processes and FC (31).

One prevalent challenge with rs-fMRI is the presence of noise, which complicates preprocessing procedures. The relatively small variation in resting-state FC exacerbates the impact of noise on the signal (32). As a result, numerous studies have focused on refining preprocessing methods, such as motion-related noise correction, physiological noise correction, and phase-based noise correction (33). For instance, Chuang et al. explored different nuisance regression techniques and the impact of motion correction, contributing to ongoing efforts to enhance the reliability of rs-fMRI and resting-state FC analysis (34).

These advancements continue to improve the robustness of rs-fMRI as a tool for investigating brain network connectivity in both healthy and diseased states.

#### B. FC of Huntington's Disease on Mice

rs-fMRI has been extensively employed as the most common method for investigating FC in cognitive and mental health disorders. It has been widely applied to studies focusing on FC in HD. The regions exhibiting specific alterations are primarily the connections between the striatum and other brain regions (35-37). Additionally, several studies have reported impairments in the dentate gyrus and the M2 cortex in HD mouse models (32, 38-40). The

regions selected for analysis in these studies are based on areas where previous research has identified significant alterations.

Seed-based research approaches have primarily focused on examining neural networks associated with HD phenotypes, particularly those related to motor and cognitive functions. Moreover, researchers have investigated the default mode network (DMN), a "task-negative" network that shows heightened activity during periods of rest. While the DMN is not directly linked to HD pathology, it has been noted to undergo early changes in other neurodegenerative diseases, particularly Alzheimer's disease.

One of the first studies involving individuals carrying the HD gene mutation used the posterior cingulate cortex, a critical component of the DMN, as a region of interest. This study revealed reduced connectivity between the posterior cingulate cortex and both the ventromedial and dorsomedial prefrontal cortices. The reduced connectivity with the ventromedial prefrontal cortex, in particular, was associated with performance on the Stroop test. Furthermore, diminished connectivity between the posterior cingulate cortex and the inferior parietal cortex was also observed. All of these regions are integral parts of the DMN, suggesting abnormal connectivity patterns during resting states in HD patients (41). However, another study using the posterior cingulate cortex as the seed region for the DMN, alongside the supplementary motor area as the seed region for the somatosensory network, found a widespread and abnormal increase in connectivity in HD. This increase in connectivity occurred before any observed volumetric decline and showed improvement in four patients who received Pridopidine treatment (42).

## C. DGE MRI for Glucose Metabolism Connectivity

Currently, there is a paucity of research on connectivity analysis based on glucose metabolism utilizing the DGE MRI signal. However, some studies have employed this technique to examine glucose uptake and metabolism under various disease conditions.

Traditionally, glucose metabolism in the brain has been investigated using positron emission tomography (PET) with <sup>18</sup>F-fluorodeoxyglucose (FDG), a radiolabeled glucose analog. This method, known as the [<sup>18</sup>F]FDG PET scan, has been validated as an effective tool for investigating glucose metabolism and uptake in neurodegenerative diseases such as HD (43, 44) and AD (45, 46). As an alternative approach, DGE MRI can detect glucose metabolism using non-toxic glucose, making it a preferable option over [<sup>18</sup>F]FDG PET (47).

Liu et al. applied the DGE MRI signal to study glucose uptake in HD, combining it with genetic biomarkers to gain insights into glucose metabolism (48). Similarly, Eleftheriou et al. introduced a combination of DGE MRI and Förster Resonance Energy Transfer (FRET)-based fiber photometry, which offers a reliable temporal response while integrating quantitative photometric techniques with tomographic approaches (49).

Although these studies used DGE MRI to investigate glucose metabolism, they primarily focused on changes in signal intensity or metabolism rate as the key metrics (50). Investigating the connectivity of glucose metabolism between different brain regions using correlation metrics could provide deeper insights into the interregional correlation of glucose uptake. Consequently, in this study, rather than examining signal intensity, we explore glucose metabolism connectivity through the use of correlation metrics.

#### III. MATERIALS AND METHODS

#### A. Animals

All experimental procedures were approved by the Institutional Animal Care and Use Committee (IACUC) at Academia Sinica (Taipei, Taiwan), and were conducted in strict accordance with their guidelines. A total of eight male WT mice and four male HD mice, including zQ175 KI and R6/2 KI strains (C57BL/6J background), were utilized for DGE MRI experiments. Male mice were specifically chosen to minimize housing-related conflicts, as sex is not considered a significant variable affecting MRI signal interpretation.

Prior to the MRI scans, the mice were fasted for approximately 8 hours, with unrestricted access to water. The mice were housed in cages with LIGNOCEL® 3–4 S as the absorbent bedding material. These cages were maintained in a controlled environment with a 12-hour light-dark cycle (7 a.m.–7 p.m. light, 7 p.m.–7 a.m. dark), an ambient temperature of  $22 \pm 2$  °C, and a relative humidity of  $55 \pm 10\%$ . Outside of the fasting period, the mice had free access to reverse osmosis water containing 0.02% HCl and were fed a chow diet (5053-PicoLab® Rodent Diet 20). During the fasting period, the chow was removed, allowing only water access.

Four distinct cohorts of C57BL/6J mice were included in the study: 15-month-old zQ175 KI mice (n = 4), 15-month-old WT mice (n = 4), 12-week-old R6/2 KI mice (n = 4), and 12-week-old WT mice (n = 4).

#### B. Imaging Acquisition

In this study, a comprehensive DGE MRI protocol was implemented using a horizontal bore 7T scanner (Bruker PharmaScan 70/16, Ettlingen, Germany) at the Animal Imaging Facility of Academia Sinica (Taipei, Taiwan). Signal transmission was achieved using an 89/72-mm volume coil, while signal reception utilized a 4-channel, receive-only mouse head coil. This setup was employed to investigate C57BL/6J mice. The acquisition protocol involved

multiple imaging sequences.

First, T2-weighted imaging (T2WI) was conducted for image registration purposes with the following parameters: repetition time (TR) = 5000 ms, echo time (TE) = 33 ms, field of view (FOV) = 16x16 mm, slice thickness = 1 mm, matrix size = 256x256, RARE factor = 8, slice number = 5, and one average, resulting in a total scan time of 2 minutes and 40 seconds. Following this, a B0 map shim was acquired prior to glucose injection.

For DGE MRI, the sequence was performed with the following parameters: TR = 65,000 ms, TE = 40.43 ms, FOV = 16x16 mm, slice thickness = 1 mm, matrix size = 128x32, RARE factor = 23, slice number = 5, RF peak amplitude = 1.6  $\mu$ T, 90 repetitions, one average, spoiling at 78.12 cycles, with a duration of 12 ms, and 20% amplitude. The interlaced object ordering mode was used. Glucose injection commenced 20 minutes into the scan, with 0.15 ml of 50% glucose administered intravenously via the tail vein over the course of one minute.

During the injection, isoflurane anesthesia was maintained at 2.5%, with breath rate monitored in two phases: 25–30 breaths per minute during the injection and 30–40 breaths per minute following the injection, with isoflurane reduced to 2.0%. This comprehensive MRI protocol facilitated an in-depth investigation of chemical exchange saturation transfer (CEST) and DGE effects in the C57BL/6J mice model.

#### C. Data Preprocessing

#### 1) Data Conversion

Bruker's 2D sequence (2dseq) serves as the standard output format for Bruker MRI data. However, for preprocessing and connectivity analysis, the NIfTI format is preferred. To address this, a data format conversion was performed using an in-house developed script in MATLAB 2018b. This process involved extracting T2-weighted imaging (T2WI) data from the binary file and reshaping the DGE MRI data to reflect the appropriate dimensions and orientation.

Additionally, the CEST data were processed to generate contrast images.

Following the adjustment of the MRI data, the converted data were saved in the NIfTI format. The NIfTI format supports a maximum of seven dimensions, with the T2WI and brain mask requiring three dimensions, and the DGE MRI data necessitating four dimensions for time-series analysis. The voxel size of the resulting NIfTI file was set to  $0.078 \times 0.078 \times 1.000$  mm with a left-posterior-inferior (LPI) orientation.

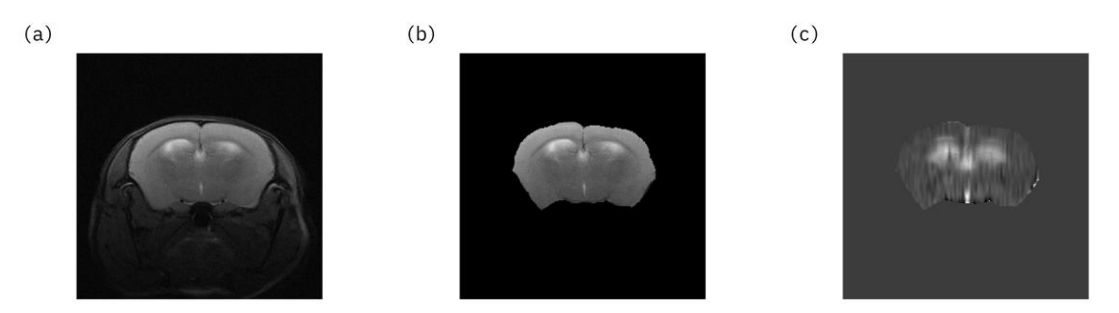


Figure 1. Example of the mice brain MRI signal. (a) T2WI (b) Masked T2WI (c) DGE MRI Source: Snapshot of applied data in this study taken by author.

#### 2) Spatial Normalization

In the process of brain MRI spatial normalization, a reference subject was selected from each group to serve as a standard for alignment. Non-linear registration was subsequently applied to align each subject's T2WI data to the selected reference subject within their respective group. Once the registration was completed, the T2WI images from each group were averaged to generate group-specific T2WI templates.

Following this, each subject's T2WI was registered to the group-wise template, ensuring consistent alignment across all subjects within each group. The final step involved registering the DGE MRI data to the template using the deformation information derived from the T2WI registration, achieving comprehensive spatial normalization. This process enabled meaningful comparisons and analyses within and across the different groups. The entire procedure was executed using a combination of AFNI software and in-house developed Python scripts.

## 3) Label Co-registration

To advance the region of interest (ROI)-based correlation analysis of glucose metabolism, signal extraction was performed using predefined atlas labels. In this study, the Australian Mouse Brain Mapping Consortium (AMBMC) atlas was utilized as the reference label. Non-linear registration was applied to the symmetric AMBMC model, aligning it with the 3D space of each group-specific template. This alignment was achieved through a combination of AFNI software and partially in-house developed Python scripts. An example of the co-registered atlas label is presented in Figure 2, illustrating the successful integration of the atlas with the group-wise templates.

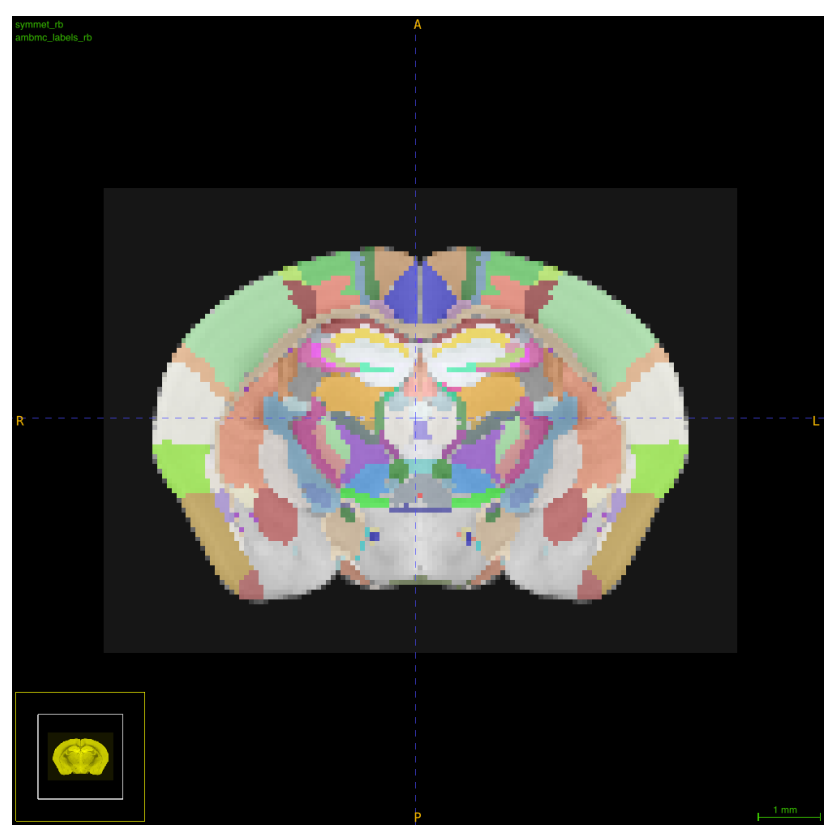


Figure 2. Registered atlas label from AMBMC.

Source: Snapshot of applied data in this study taken by author.

The labels were split into the following contours: anterior cerebral artery (ACA), dentate gyrus (DG), hippocampus, retrosplenial cortex (RSP), thalamic, caudate putamen (CPu),

insular region (Ins), primary somatosensory cortex (S1), secondary somatosensory cortex (S2), primary motor cortex (M1), secondary somatosensory cortex (M2), central amygdaloid nucleus (Ce), temporal association area (TeA), and complete thalamus, while each contour is divided into left and right hemisphere.

#### D. Connectivity Analysis of Glucose Metabolism

To evaluate glucose metabolism connectivity, we performed ROI-based connectivity analysis, focusing on specific ROIs associated with the pathology of HD. The selected regions are detailed in Table 1.

For each subject and each ROI, we extracted the time series of the region-averaged BOLD signal. Pearson correlation coefficients were then calculated between the BOLD signal time series of each pair of ROIs. These correlation values were Fisher Z-transformed to generate subject-specific connectivity matrices. This process was repeated for each subject across different age groups, allowing for comprehensive analysis of age-related changes in connectivity.

## E. Statistical Analysis

For ROI-based connectivity analysis, significant connections within each group (One-sample t-test,  $p \le 0.05$ , False Discovery Rate (FDR) corrected) were identified, and between-group connectivity differences were tested for pairs found to be significantly different in at least one of the groups (two-sample t-test, FDR corrected,  $p \le 0.05$ ). The statistics procedures above were performed in MATLAB R2018b.

Table 1. Brain regions and abbreviations

Source: Organized by author.

Region	Structure	
Cingulate region	ACA	Anterior cerebral artery (A24a, A24a', A24b, A24b')
	RSP	Retrosplenial cortex (A29a, A29b, A29c, A30)
Somatosensory cortex	S1	Primary somatosensory cortex
	S2	Secondary somatosensory cortex
Motor cortex	M1	Primary motor cortex
	M2	Secondary motor cortex
Insular region	Ins	Insular region, not subdivided
Temporal region	TeA	Temporal association area
Hippocampus	DG	Dentate gyrus
Associated structure	Ce	Central amygdaloid nucleus
Corpus striatum	CPu	Caudate putamen
Diencephalon		Thalamus

#### F. Curve Clustering Analysis

To analyze glucose metabolism connectivity, we employed a self-organizing map (SOM), an unsupervised neural network model that projects high-dimensional data onto a two-dimensional grid while preserving topological relationships (51). This technique clusters similar data points, allowing for a meaningful spatial representation of temporal signal patterns in DGE MRI images.

For this study, pixel-level time curves from MRI images were extracted, reshaped, and flattened for SOM input. A 5x6 SOM grid was trained 200 epochs to classify temporal profiles into distinct clusters, which were subsequently visualized as spatial heatmaps over the brain's anatomical regions.

The resulting clusters, each representing similar time-series curves, were averaged to identify dominant glucose uptake patterns. These clusters were also compared across subjects, allowing to observe variability in metabolic activity and potential markers of dysfunction.

#### IV. RESULTS

Pearson correlation matrices were computed from the DGE MRI signal for each ROI mentioned in the previous chapter, separately for the left and right hemispheres. An example of the DGE MRI signal is provided in Figure 3. For each group, the average DGE MRI signal for every region was calculated across all subjects, providing a representative measure of glucose metabolism connectivity within each hemisphere.

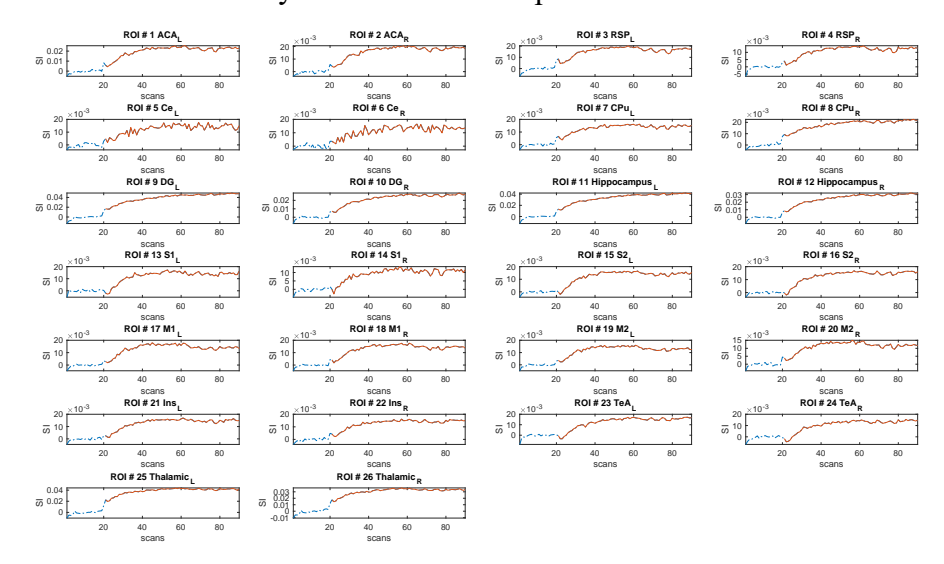


Figure 3. Averaged DGE MRI signal for the selected ROIs on the left and right hemispheres of zQ175 KI mice.

Source: Illustrated by author.

# A. zQ175 KI Mice

The Pearson correlation for each selected ROI of WT mice (15 m.o.) and zQ175 KI mice (15 m.o.) was calculated in this analysis. The averaged Pearson correlation for both groups is shown in Figure 4.

To find the alteration of the glucose metabolism connectivity, the two-sample t-test was done (FDR corrected,  $p \le 0.05$ ). Kim et al previously mentioned that the CEST contrast increases almost constant for glucose over the 30 min period of observation (52). Therefore, the DGE MRI signal was split into several sections: 21-90 mins (complete data), 21-50 mins (first section), and 51-90 mins (second section), note that the first 20 minutes of DGE MRI is considered as the baseline of glucose uptake. The p-value matrix is shown in Figure 5.

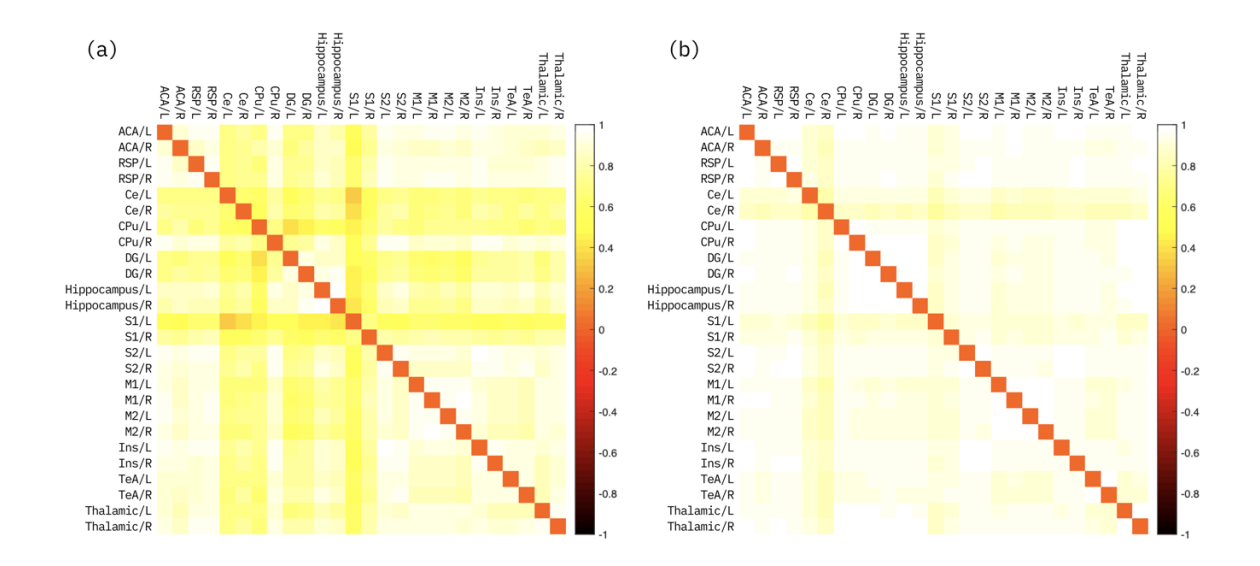


Figure 4. Pearson correlation matrices of 15 m.o. WT and zQ175 KI mice. Source: Illustrated by author.

(a) Average of WT mice Pearson correlation matrix; (b) Average of zQ175 KI mice Pearson correlation matrix.

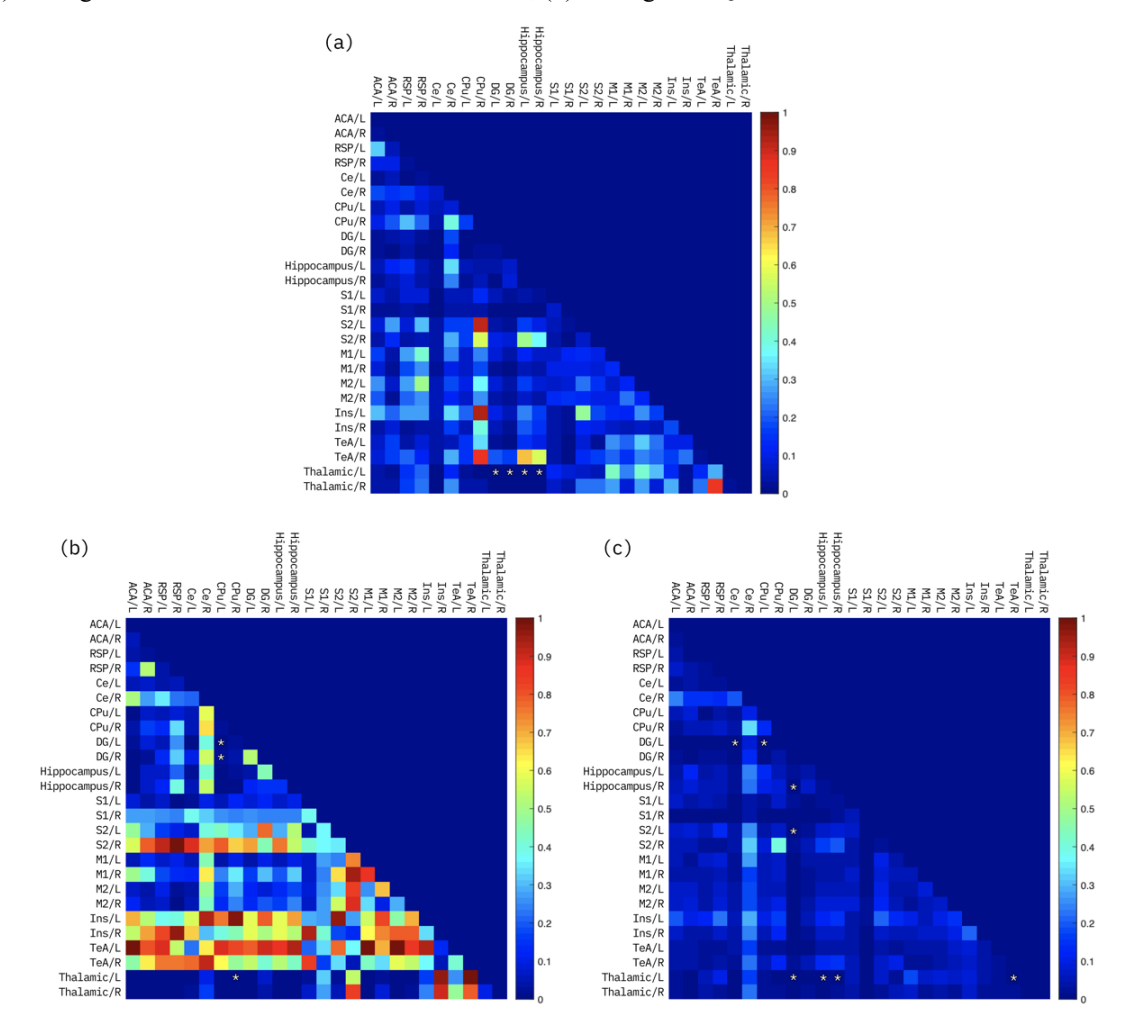


Figure 5. p-value matrix from two-sample t-test result of WT and zQ175 KI mice (\*= $p \le 0.05$ , FDR corrected).

(a) Time points: 21-90 mins (b) Time points: 21-50 mins (c) Time points: 51-90 mins Source: Illustrated by author.

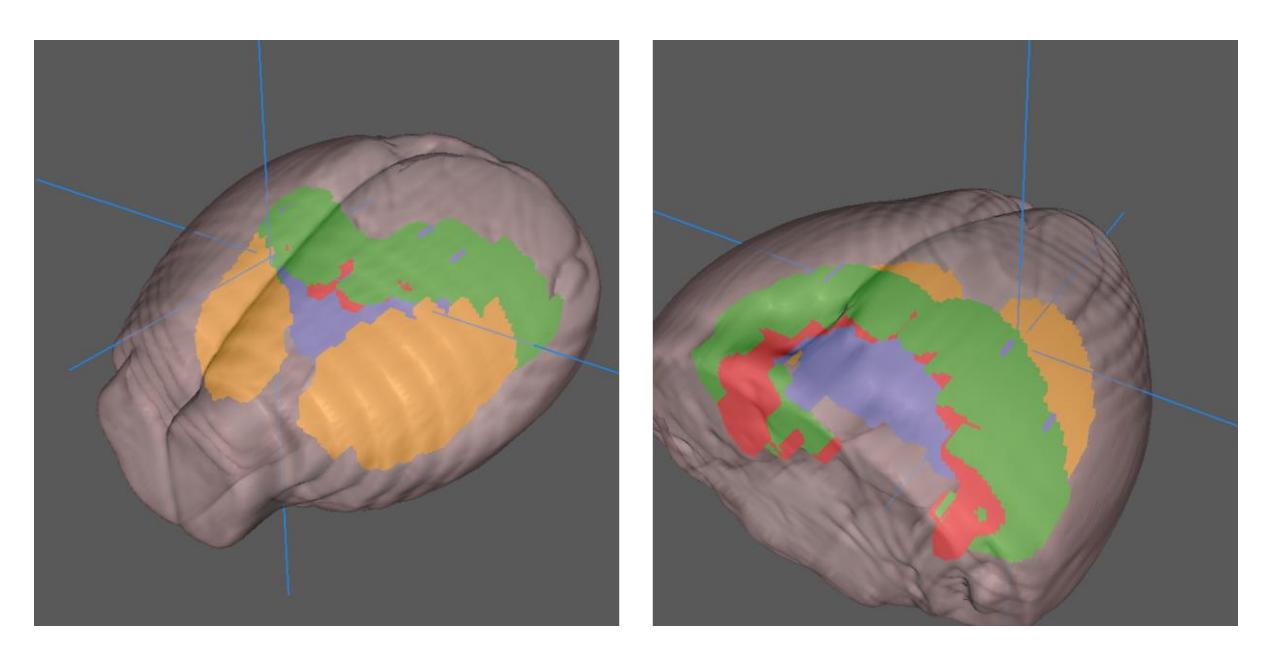


Figure 6. 3D-rendered ROI with significant alteration in two-sample t-test of WT and zQ175 KI mice. red: dentate gyrus (DG); green: hippocampus; blue: thalamus; yellow: caudate putamen (CPu)

Source: Illustrated & rendered by author.

#### B. R6/2 KI Mice

Following the same procedure of zQ175 KI mice, the analysis was done on WT mice (13 weeks old) and R6/2 KI mice (13 weeks old). The average Pearson correlation for both groups is shown in Figure 7, where the p-value matrix of the two-sample t-test (FDR corrected,  $p \le 0.05$ ) within different sections of the signal is as shown in Figure 8. From the first section (21-50 mins), several significant alterations were found between different regions of the thalamus, such as ACA, RSP, hippocampus, and the motor cortex. However, a significant alternation was found in the correlation between CPu and DG, which aligns with the pathology of impaired brain regions.

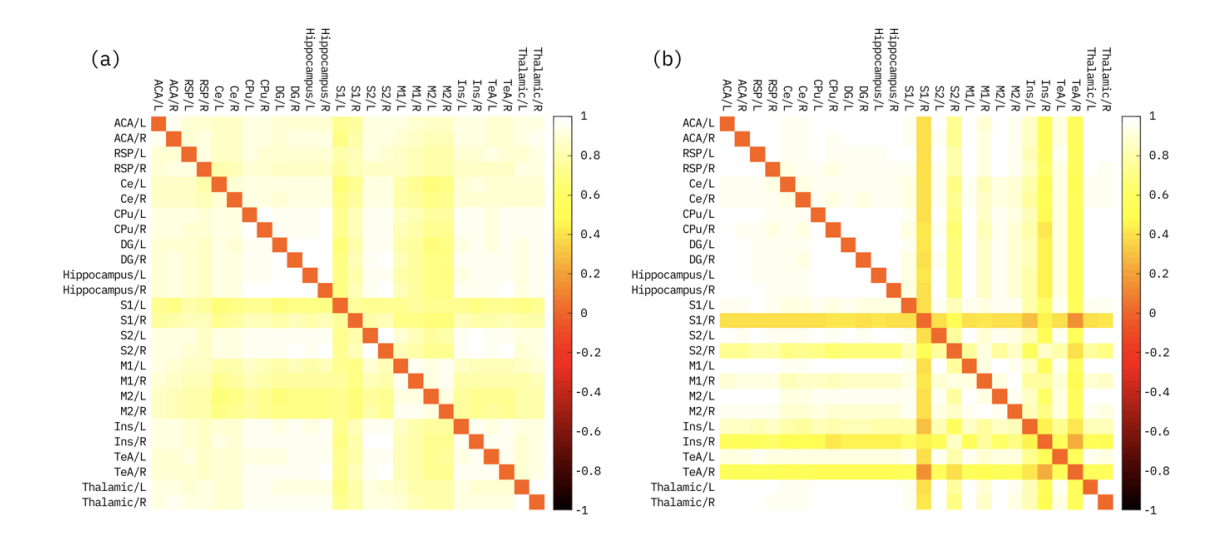


Figure 7. Pearson correlation matrices of 13-week-old WT and R6/2 KI mice. Source: Illustrated by author.

(a) Average of WT mice Pearson correlation; (b) Average of R6/2 mice Pearson correlation.

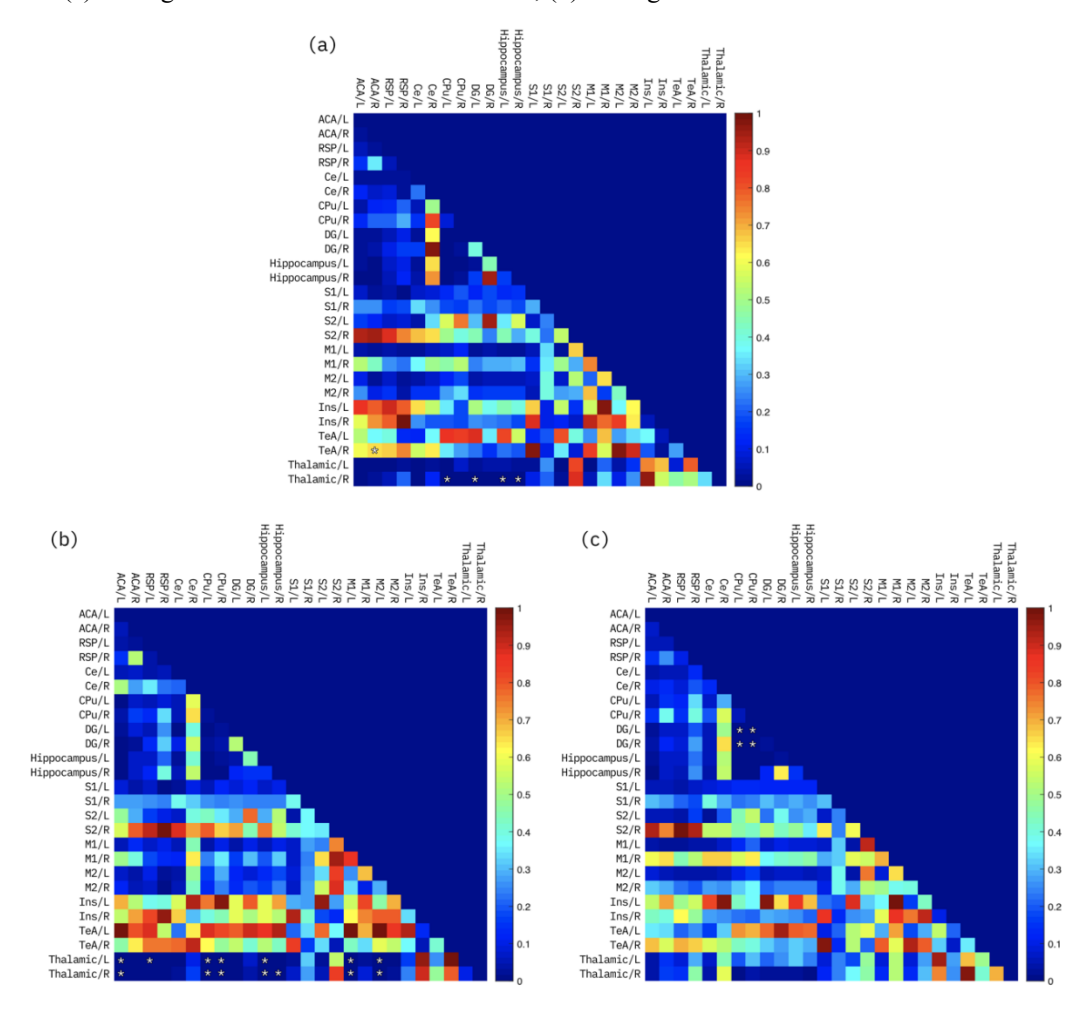


Figure 8. p-value matrix from two-sample t-test result of WT and R6/2 mice (\*=p  $\leq$  0.05, FDR corrected). (a) Time points: 21-90 mins (b) Time points: 21-50 mins (c) Time points: 51-90 mins Source: Illustrated by author.

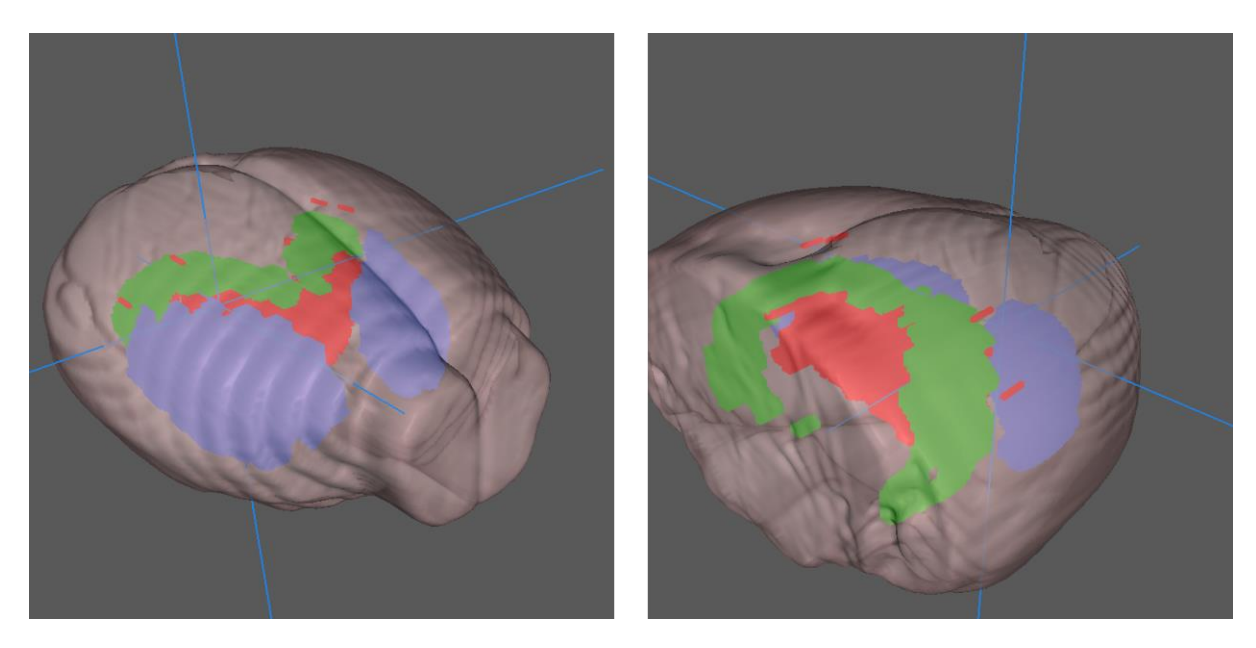


Figure 9. 3D-rendered ROI with significant alteration in two-sample t-test of WT and R6/2 KI mice. red: thalamus; green: dentate gyrus (DG); blue: caudate putamen (CPu)

Source: Illustrated & rendered by author.

# C. Curve Clustering Analysis

The curve clustering analysis of DGE MRI data was performed using self-organizing maps (SOM) after 200 training epochs. Figure 10 and Figure 11 presents the discrete clustering results, where different categories represent distinct regions of metabolic activity. Each color corresponds to a specific cluster, indicating areas of the brain that share similar glucose metabolism patterns. These discrete clusters highlight the regions with similar metabolic connectivity, without reference to anatomical slices. The spatial distribution of these clusters suggests the presence of distinct metabolic zones, where certain regions demonstrate a cohesive glucose metabolism behavior.

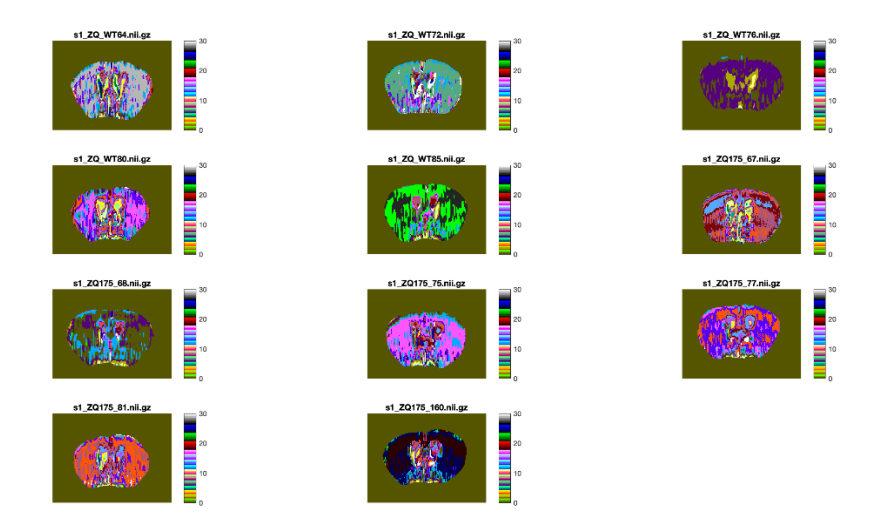


Figure 10. SOM clustered voxel DGE MRI signal of 15 m.o. WT and zQ175 KI mice. Source: Illustrated by author.

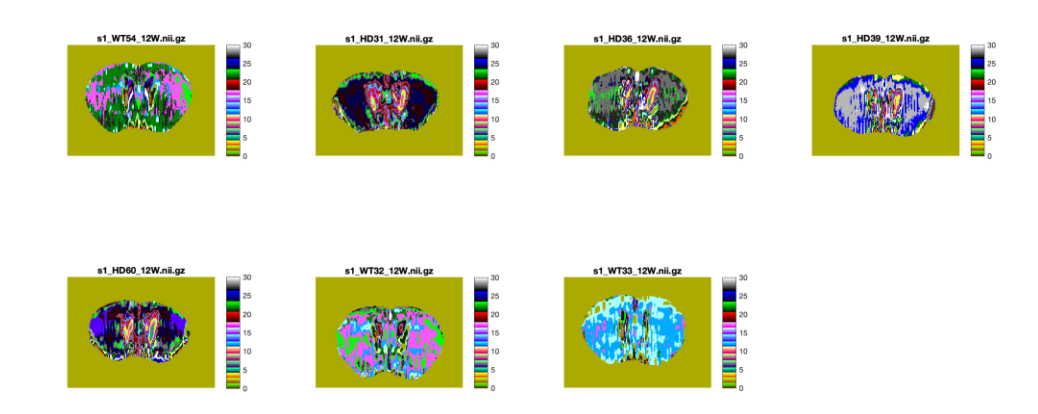


Figure 11. SOM clustered voxel DGE MRI signal of 12 weeks old WT and R6/2 KI mice. Source: Illustrated by author.

In Figure 12 and Figure 13, the curves represent the averaged signal for each identified cluster. These curves summarize the glucose metabolism dynamics within the corresponding clustered regions. Across the clusters, various patterns emerge: some regions show an initial rapid increase in signal strength, followed by a steady plateau, while others exhibit more gradual and consistent changes over time. These averaged curves provide a temporal snapshot of glucose metabolism within each cluster, offering a clearer understanding of the distinct metabolic characteristics of each region.

The clustering analysis reveals a clear distinction between the metabolic behaviors of different brain regions, with discrete categorization helping to identify patterns that may not be apparent in raw image data. These results demonstrate the efficacy of SOM in clustering and analyzing DGE MRI data, offering insights into the spatial and temporal diversity of glucose metabolism.

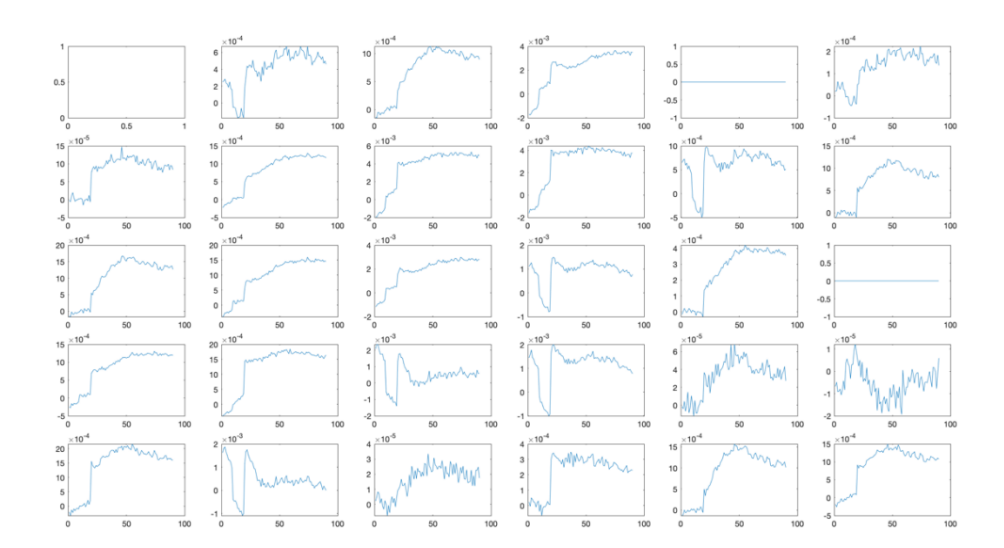


Figure 12. Averaged DGE MRI signal of SOM clustered voxel groups of 15 m.o. WT and zQ175 KI mice. Source: Illustrated by author.

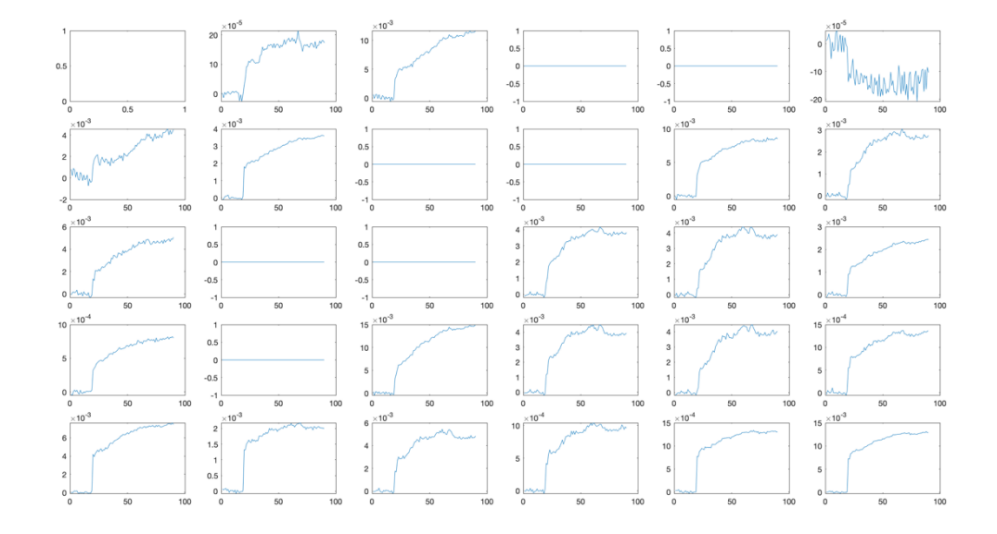


Figure 13. Averaged DGE MRI signal of SOM clustered voxel groups of 12 weeks old WT and R6/2 KI mice. Source: Illustrated by author.

#### V. DISCUSSION

This study explores the potential of DGE MRI as a novel approach to assess glucose metabolism connectivity in HD, using two commonly employed mouse models, zQ175 KI and R6/2 KI. While HD is widely associated with motor, cognitive, and psychiatric symptoms, there is an increasing interest in examining its metabolic disturbances, which may serve as valuable clinical biomarkers (4, 5). Traditional methods for assessing glucose metabolism, such as MRS, have been supplemented by advancements in DGE MRI, which allows for more precise and efficient monitoring of brain glucose levels (8-11).

Our findings indicate that zQ175 KI mice exhibit significant alterations in glucose metabolism connectivity. Using Pearson correlation analysis, we identified brain regions with notably distinct connectivity profiles in DGE MRI signals compared to WT mice. This suggests certain brain areas may be more susceptible to metabolic changes, offering key insights into HD pathophysiology. Affected regions included the thalamus, caudate putamen, central amygdaloid nucleus, and dentate gyrus, all associated with HD-related volume loss and functional impairments (see Figure 4 and Figure 5) (39, 40, 53-55).

Similarly, analysis of R6/2 KI mice revealed altered glucose metabolism connectivity. Here, Pearson correlation analysis highlighted distinct connectivity patterns in multiple brain regions compared to WT mice, with these differences manifesting across various time points in the DGE MRI signal. The connectivity patterns in R6/2 KI mice showed similarities to those of zQ175 KI mice, except for the thalamus, which displayed more prominent connectivity variations with cortical regions, such as the M1 and M2 cortices (see Figure 7 and Figure 8).

The thalamus, which transmits sensory information to different cerebral cortex areas, is fundamental in regulating consciousness, alertness, and sensory input processing (56). The caudate putamen, part of the striatum, plays a critical role in movement control and is also involved in cognitive functions such as decision-making and reward processing. The central

amygdaloid nucleus, part of the amygdala, is deeply connected to emotional processing, especially fear and anxiety (57). The dentate gyrus, a hippocampal structure, contributes primarily to memory formation and spatial navigation. Each of these brain regions is thus associated with cognitive, sensory, or memory-related functions (58).

Our study utilized the R6/2 KI and zQ175 KI models of HD. The R6/2 model is distinguished by pronounced HD-related pathology, including motor dysfunction, inclusion body formation, and premature mortality. Given the disease's rapid progression, R6/2 mice are often used as models for juvenile-onset HD, with a life expectancy of around 15 weeks due to the aggressive onset of symptoms. In contrast, zQ175 KI mice show mHTT nuclear staining and aggregates in the striatum and cortex, which become significant by four months of age (59). By comparing these models, we observed more pronounced alterations in thalamus-cortex connectivity in R6/2 mice, which may arise earlier and with greater severity due to their accelerated disease progression. In contrast, the slower disease progression in zQ175 KI mice may reflect different patterns of thalamus-cortex connectivity changes over time (60).

While multiple approaches, such as amplitude of low-frequency fluctuation (ALFF) (61) and nuisance regression (62), can be applied to resting-state FC analysis, limitations inherent to DGE MRI restrict their use in this study. Nuisance regression, typically used for noise reduction, motion correction, and signal detrending, is incompatible with DGE MRI, where signals reflect glucose chemical exchange trends. Future studies should focus on DGE MRI pre-processing methods for glucose metabolism and FC analysis to further evaluate DGE MRI's utility as an HD biomarker.

The application of SOM in clustering DGE MRI data offers a unique framework for identifying distinct metabolic connectivity patterns across brain regions. The clustering analysis, highlighted in Figure 10 to Figure 13, emphasizes SOM's potential in distinguishing brain areas that share similar glucose metabolism dynamics. By organizing these regions into discrete clusters, this method goes beyond traditional anatomical mapping, enabling a fresh

perspective on glucose metabolic zones and their cohesive behaviors. The averaged curves in Figures 12 and 13 bring to light the unique temporal patterns of each cluster, revealing metabolic behaviors that could be overlooked in raw DGE MRI data. Some clusters display sharp initial increases followed by stable plateaus, while others show more gradual changes in signal over time. This clustering analysis thus uncovers subtle spatial and temporal variations in glucose metabolism, offering new insights into metabolic shifts that may be relevant to the progression of neurodegenerative diseases such as HD.

However, the complexity of SOM mapping within DGE MRI data presents substantial analytical challenges. Although SOM effectively clusters regions with similar glucose dynamics, interpreting these clusters is not straightforward. The resulting features often lack clear definitions, partly due to the inherently low signal strength in the small structures of the mice brain. This limitation in signal-to-noise ratio (SNR) makes it difficult to delineate specific metabolic characteristics within each cluster accurately, introducing ambiguity in the spatial and temporal trends identified.

Further, the promise of identifying diagnostic biomarkers based on glucose metabolism patterns in specific brain regions is still largely aspirational. The observed curve patterns—whether they exhibit rapid initial increases, gradual changes, or other dynamics—highlight potential, but the variability in these signals requires rigorous study. To fully understand whether these patterns could serve as reliable biomarkers, further investigation is needed into both metabolic processes and neural network training methods. Such efforts would enhance the precision of SOM-based clustering and help clarify whether these distinct glucose metabolism zones are genuinely reflective of underlying disease mechanisms, particularly in neurodegenerative disorders like HD. Thus, while SOM clustering offers intriguing insights, its potential as a diagnostic tool is contingent on deeper, methodical research into both the biological significance and analytical robustness of these metabolic patterns.

#### VI. CONCLUSION

While DGE MRI has been widely utilized for assessing glucose metabolism, its application in connectivity analysis as an index of energy utilization in HD patients remains unexplored and requires proof of concept from various perspectives. This study leverages the zQ175 KI and R6/2 KI mouse models to investigate glucose metabolism connectivity in HD, revealing potential disruptions within specific brain regions. Notably, our analysis highlights distinct connectivity disruptions, particularly between the striatum and dentate gyrus and in thalamic-cortical pathways, where the findings are consistent with established HD pathology and suggest that DGE MRI could be sensitive to early metabolic connectivity changes.

However, validating these findings requires additional studies, including isotopically labeled (2-deoxy-D-glucose) 2DG, which is an established method for measuring glucose metabolism. Unlike glucose, 2DG enters cells via the same transporters as glucose and is phosphorylated but minimally metabolized further, allowing it to act as a stable tracer of glucose uptake. By comparing results of glucose with 2DG, we can more accurately determine how well DGE MRI reflects actual glucose metabolism and clarify its sensitivity to metabolic connectivity changes. Additionally, fiber photometry could enable real-time recording of neural activity through calcium or neurotransmitter signaling, offers a complementary approach to assess FC and neuronal dynamics in HD. Together, these methods provide a more robust framework to evaluate and validate DGE MRI's reliability and specificity as a tool for mapping metabolic connectivity changes, potentially solidifying its role in HD diagnosis and monitoring.

By linking metabolic alterations to specific connectivity patterns in HD, our study proposes DGE MRI as a promising approach to enhance our understanding of HD pathogenesis and as a potential biomarker for early diagnosis and disease monitoring. This research establishes a foundational framework for further exploration, advancing prospects for targeted therapies that address metabolic dysregulation in HD.

#### VII. REFERENCES

- 1. Kuwert T, Lange HW, Langen KJ, Herzog H, Aulich A, Feinendegen LE. Cerebral glucose consumption measured by PET in patients with and without psychiatric symptoms of Huntington's disease. Psychiatry Research. 1989;29(3):361-2. doi: https://doi.org/10.1016/0165-1781(89)90090-5.
- 2. Conner LT, Srinageshwar B, Bakke JL, Dunbar GL, Rossignol J. Advances in stem cell and other therapies for Huntington's disease: An update. Brain Research Bulletin. 2023;199:110673. doi: https://doi.org/10.1016/j.brainresbull.2023.110673.
- 3. Cavanna AE. Huntington Disease. Motion and Emotion: The Neuropsychiatry of Movement Disorders and Epilepsy. Cham: Springer International Publishing; 2018. p. 93-9.
- 4. Chaves G, Özel RE, Rao NV, Hadiprodjo H, Costa YD, Tokuno Z, et al. Metabolic and transcriptomic analysis of Huntington's disease model reveal changes in intracellular glucose levels and related genes. Heliyon. 2017;3(8):e00381. doi: https://doi.org/10.1016/j.heliyon.2017.e00381.
- 5. De Volder A, Bol A, Michel C, Cogneau M, Evrard P, Lyon G, et al. Brain glucose utilization in childhood Huntington's disease studied with positron emission tomography (PET). Brain and Development. 1988;10(1):47-50. doi: <a href="https://doi.org/10.1016/S0387-7604(88)80046-9">https://doi.org/10.1016/S0387-7604(88)80046-9</a>.
- 6. Rao J, Oz G, Seaquist ER. Regulation of cerebral glucose metabolism. Minerva Endocrinol. 2006;31(2):149-58. Epub 2006/05/10. PubMed PMID: 16682938.
- 7. Boddie AW, Frazer JW, Tomasovic SP, Dennis L. Application of MR spectroscopy to the study of tumor biology. Journal of Surgical Research. 1989;46(1):90-7. doi: <a href="https://doi.org/10.1016/0022-4804(89)90186-8">https://doi.org/10.1016/0022-4804(89)90186-8</a>.
- 8. Huang J-Y, Peng S-F, Yang C-C, Yen K-Y, Tzen K-Y, Yen R-F. Neuroimaging Findings in a Brain With Niemann–Pick Type C Disease. Journal of the Formosan Medical Association. 2011;110(8):537-42. doi: https://doi.org/10.1016/S0929-6646(11)60080-6.
- 9. Dona AC, Pages G, Kuchel PW. Kinetics of starch hydrolysis and glucose mutarotation studied by NMR chemical exchange saturation transfer (CEST). Carbohydrate Polymers. 2011;86(4):1525-32. doi: https://doi.org/10.1016/j.carbpol.2011.06.056.
- 10. Law LH, Huang J, Xiao P, Liu Y, Chen Z, Lai JHC, et al. Multiple CEST contrast imaging of nose-to-brain drug delivery using iohexol liposomes at 3T MRI. Journal of Controlled Release. 2023;354:208-20. doi: https://doi.org/10.1016/j.jconrel.2023.01.011.
- 11. Schache D, Bardin S, Ciobanu L, Faber C, Hoerr V. Ultrafast CEST line scanning as a method to quantify mutarotation kinetics. Journal of Magnetic Resonance. 2022;342:107270. doi: <a href="https://doi.org/10.1016/j.jmr.2022.107270">https://doi.org/10.1016/j.jmr.2022.107270</a>.
- 12. Biswal B, Zerrin Yetkin F, Haughton VM, Hyde JS. Functional connectivity in the motor cortex of resting human brain using echo-planar mri. Magnetic Resonance in Medicine.

- 1995;34(4):537-41. doi: <a href="https://doi.org/10.1002/mrm.1910340409">https://doi.org/10.1002/mrm.1910340409</a>.
- 13. Shokri-Kojori E, Tomasi D, Alipanahi B, Wiers CE, Wang G-J, Volkow ND. Correspondence between cerebral glucose metabolism and BOLD reveals relative power and cost in human brain. Nature Communications. 2019;10(1):690. doi: 10.1038/s41467-019-08546-x.
- 14. Kallimorou C, Platoni K, Christidi F, Mantonakis L, Spilioti E, Velonakis G, et al. P.5.9 CAN INTRINSIC CONNECTIVITY CONTRAST RS-FMRI INDEX IDENTIFY FUNCTIONAL CHANGES IN SCHIZOPHRENIA? Physica Medica. 2022;104:S46-S7. doi: https://doi.org/10.1016/S1120-1797(22)03148-9.
- 15. Kirino E, Tanaka S, Nagai Y, Usui C, Inami R, Inoue R. S14-4 Abnormality of functional connectivity in schizophrenia evaluated using simultaneous rs-fMRI and EEG recordings. Clinical Neurophysiology. 2020;131(10):e252. doi: <a href="https://doi.org/10.1016/j.clinph.2020.04.092">https://doi.org/10.1016/j.clinph.2020.04.092</a>.
- 16. Roig-Herrero A, Planchuelo-Gómez Á, Hernández-García M, de Luis-García R, Fernández-Linsenbarth I, Beño-Ruiz-de-la-Sierra RM, et al. Default mode network components and its relationship with anomalous self-experiences in schizophrenia: A rs-fMRI exploratory study. Psychiatry Research: Neuroimaging. 2022;324:111495. doi: <a href="https://doi.org/10.1016/j.pscychresns.2022.111495">https://doi.org/10.1016/j.pscychresns.2022.111495</a>.
- 17. Ruiz-Torras S, Gudayol-Ferré E, Fernández-Vazquez O, Cañete-Massé C, Peró-Cebollero M, Guàrdia-Olmos J. Hypoconnectivity networks in schizophrenia patients: A voxel-wise meta-analysis of Rs-fMRI. International Journal of Clinical and Health Psychology. 2023;23(4):100395. doi: https://doi.org/10.1016/j.ijchp.2023.100395.
- 18. Wang L-X, Guo F, Zhu Y-Q, Wang H-N, Liu W-M, Li C, et al. Effect of second-generation antipsychotics on brain network topology in first-episode schizophrenia: A longitudinal rs-fMRI study. Schizophrenia Research. 2019;208:160-6. doi: https://doi.org/10.1016/j.schres.2019.03.015.
- 19. Yu T, Li Y, Li N, Huang J, Fan F, Luo X, et al. Regional Homogeneity in schizophrenia patients with tardive dyskinesia: a resting-state fMRI study. Psychiatry Research: Neuroimaging. 2023;335:111724. doi: <a href="https://doi.org/10.1016/j.pscychresns.2023.111724">https://doi.org/10.1016/j.pscychresns.2023.111724</a>.
- 20. Araújo RP, Figueiredo P, Pinto J, Vilela P, Martins IP, Gil-Gouveia R. Altered functional connectivity in a sensorimotor-insular network during spontaneous migraine attacks: A resting-state FMRI study. Brain Research. 2023;1818:148513. doi: <a href="https://doi.org/10.1016/j.brainres.2023.148513">https://doi.org/10.1016/j.brainres.2023.148513</a>.
- 21. Liu L, Lyu T-L, Fu M-Y, Wang L-P, Chen Y, Hong J-H, et al. Changes in brain connectivity linked to multisensory processing of pain modulation in migraine with acupuncture treatment. NeuroImage: Clinical. 2022;36:103168. doi: https://doi.org/10.1016/j.nicl.2022.103168.
- 22. Martinelli D, Castellazzi G, De Icco R, Bitetto V, Allena M, Ahmad L, et al. Altered

- thalamo cortical connectivity in episodic migraine: A resting state exploratory FMRI study. Journal of the Neurological Sciences. 2021;429:119297. doi: https://doi.org/10.1016/j.jns.2021.119297.
- 23. Agosta F, Pievani M, Geroldi C, Copetti M, Frisoni GB, Filippi M. Resting state fMRI in Alzheimer's disease: beyond the default mode network. Neurobiology of Aging. 2012;33(8):1564-78. doi: https://doi.org/10.1016/j.neurobiologing.2011.06.007.
- 24. Dimitriadis SI. Quantifying the predictive power of resting-state functional connectivity (rs-fc) fMRI for identifying patients with Alzheimer's disease (AD). Clinical Neurophysiology. 2015;126(11):2043-4. doi: https://doi.org/10.1016/j.clinph.2015.03.011.
- 25. Marchitelli R, Aiello M, Cachia A, Quarantelli M, Cavaliere C, Postiglione A, et al. Simultaneous resting-state FDG-PET/fMRI in Alzheimer Disease: Relationship between glucose metabolism and intrinsic activity. NeuroImage. 2018;176:246-58. doi: https://doi.org/10.1016/j.neuroimage.2018.04.048.
- 26. Wei W, Zhang K, Chang J, Zhang S, Ma L, Wang H, et al. Analyzing 20 years of Resting-State fMRI Research: Trends and collaborative networks revealed. Brain Research. 2024;1822:148634. doi: <a href="https://doi.org/10.1016/j.brainres.2023.148634">https://doi.org/10.1016/j.brainres.2023.148634</a>.
- 27. Claeys EHI, Mantingh T, Morrens M, Yalin N, Stokes PRA. Resting-state fMRI in depressive and (hypo)manic mood states in bipolar disorders: A systematic review. Progress in Neuro-Psychopharmacology and Biological Psychiatry. 2022;113:110465. doi: https://doi.org/10.1016/j.pnpbp.2021.110465.
- 28. Dai P, Lu D, Shi Y, Zhou Y, Xiong T, Zhou X, et al. Classification of recurrent major depressive disorder using a new time series feature extraction method through multisite rs-fMRI data. Journal of Affective Disorders. 2023;339:511-9. doi: <a href="https://doi.org/10.1016/j.jad.2023.07.077">https://doi.org/10.1016/j.jad.2023.07.077</a>.
- 29. Li W, Wang C, Lan X, Fu L, Zhang F, Ye Y, et al. Variability and concordance among indices of brain activity in major depressive disorder with suicidal ideation: A temporal dynamics resting-state fMRI analysis. Journal of Affective Disorders. 2022;319:70-8. doi: https://doi.org/10.1016/j.jad.2022.08.122.
- 30. Nawaz H, Shah I, Ali S. The amygdala connectivity with depression and suicide ideation with suicide behavior: A meta-analysis of structural MRI, resting-state fMRI and task fMRI. Progress in Neuro-Psychopharmacology and Biological Psychiatry. 2023;124:110736. doi: https://doi.org/10.1016/j.pnpbp.2023.110736.
- 31. Lv H, Wang Z, Tong E, Williams LM, Zaharchuk G, Zeineh M, et al. Resting-State Functional MRI: Everything That Nonexperts Have Always Wanted to Know. American Journal of Neuroradiology. 2018;39(8):1390-9. doi: 10.3174/ajnr.A5527.
- 32. Raimondo L, Oliveira ÍAF, Heij J, Priovoulos N, Kundu P, Leoni RF, et al. Advances in resting state fMRI acquisitions for functional connectomics. NeuroImage. 2021;243:118503. doi: <a href="https://doi.org/10.1016/j.neuroimage.2021.118503">https://doi.org/10.1016/j.neuroimage.2021.118503</a>.

- 33. De Blasi B, Caciagli L, Storti SF, Galovic M, Koepp M, Menegaz G, et al. Noise removal in resting-state and task fMRI: functional connectivity and activation maps. Journal of Neural Engineering. 2020;17(4):046040. doi: 10.1088/1741-2552/aba5cc.
- 34. Chuang K-H, Lee H-L, Li Z, Chang W-T, Nasrallah FA, Yeow LY, et al. Evaluation of nuisance removal for functional MRI of rodent brain. NeuroImage. 2019;188:694-709. doi: <a href="https://doi.org/10.1016/j.neuroimage.2018.12.048">https://doi.org/10.1016/j.neuroimage.2018.12.048</a>.
- 35. Seibert TM, Majid DSA, Aron AR, Corey-Bloom J, Brewer JB. Stability of resting fMRI interregional correlations analyzed in subject-native space: A one-year longitudinal study in healthy adults and premanifest Huntington's disease. NeuroImage. 2012;59(3):2452-63. doi: https://doi.org/10.1016/j.neuroimage.2011.08.105.
- 36. Vasilkovska T, Adhikari MH, Van Audekerke J, Salajeghe S, Pustina D, Cachope R, et al. Resting-state fMRI reveals longitudinal alterations in brain network connectivity in the zQ175DN mouse model of Huntington's disease. Neurobiology of Disease. 2023;181:106095. doi: https://doi.org/10.1016/j.nbd.2023.106095.
- 37. Liu W, Yang J, Chen K, Luo C, Burgunder J, Gong Q, et al. Resting-state fMRI reveals potential neural correlates of impaired cognition in Huntington's disease. Parkinsonism & Related Disorders. 2016;27:41-6. doi: <a href="https://doi.org/10.1016/j.parkreldis.2016.04.017">https://doi.org/10.1016/j.parkreldis.2016.04.017</a>.
- 38. Fedele V, Roybon L, Nordström U, Li JY, Brundin P. Neurogenesis in the R6/2 mouse model of Huntington's disease is impaired at the level of NeuroD1. Neuroscience. 2011;173:76-81. doi: https://doi.org/10.1016/j.neuroscience.2010.08.022.
- 39. Phillips W, Morton AJ, Barker RA. Abnormalities of Neurogenesis in the R6/2 Mouse Model of Huntington's Disease Are Attributable to the <em>In Vivo</em> Microenvironment. The Journal of Neuroscience. 2005;25(50):11564-76. doi: 10.1523/jneurosci.3796-05.2005.
- 40. Blumenstock S, Dudanova I. Cortical and Striatal Circuits in Huntington's Disease. Frontiers in Neuroscience. 2020;14. doi: 10.3389/fnins.2020.00082.
- 41. Quarantelli M, Salvatore E, Giorgio SMDA, Filla A, Cervo A, Russo CV, et al. Default-Mode Network Changes in Huntington's Disease: An Integrated MRI Study of Functional Connectivity and Morphometry. PLOS ONE. 2013;8(8):e72159. doi: 10.1371/journal.pone.0072159.
- 42. Sánchez-Castañeda C, de Pasquale F, Caravasso CF, Marano M, Maffi S, Migliore S, et al. Resting-state connectivity and modulated somatomotor and default-mode networks in Huntington disease. CNS Neuroscience & Therapeutics. 2017;23(6):488-97. doi: https://doi.org/10.1111/cns.12701.
- 43. Andrew F, Klaus LL, James RM, John M, Gabriella K, Phoebe S, et al. Metabolic Network Abnormalities in Early Huntington's Disease: An [<sup&gt;18&lt;/sup&gt;F]FDG PET Study. Journal of Nuclear Medicine. 2001;42(11):1591.

- 44. Michels S, Buchholz H-G, Rosar F, Heinrich I, Hoffmann MA, Schweiger S, et al. 18F-FDG PET/CT: an unexpected case of Huntington's disease. BMC Neurology. 2019;19(1):78. doi: 10.1186/s12883-019-1311-9.
- 45. Chételat G, Arbizu J, Barthel H, Garibotto V, Law I, Morbelli S, et al. Amyloid-PET and (18)F-FDG-PET in the diagnostic investigation of Alzheimer's disease and other dementias. Lancet Neurol. 2020;19(11):951-62. Epub 2020/10/26. doi: 10.1016/s1474-4422(20)30314-8. PubMed PMID: 33098804.
- 46. Smailagic N, Lafortune L, Kelly S, Hyde C, Brayne C. 18F-FDG PET for Prediction of Conversion to Alzheimer's Disease Dementia in People with Mild Cognitive Impairment: An Updated Systematic Review of Test Accuracy. J Alzheimers Dis. 2018;64(4):1175-94. Epub 2018/07/17. doi: 10.3233/jad-171125. PubMed PMID: 30010119; PubMed Central PMCID: PMCPMC6218118.
- 47. Huang J, van Zijl PCM, Han X, Dong CM, Cheng GWY, Tse KH, et al. Altered d-glucose in brain parenchyma and cerebrospinal fluid of early Alzheimer's disease detected by dynamic glucose-enhanced MRI. Sci Adv. 2020;6(20):eaba3884. Epub 2020/05/20. doi: 10.1126/sciadv.aba3884. PubMed PMID: 32426510; PubMed Central PMCID: PMCPMC7220384.
- 48. Liu H, Chen L, Zhang C, Liu C, Li Y, Cheng L, et al. Interrogation of dynamic glucose-enhanced MRI and fluorescence-based imaging reveals a perturbed glymphatic network in Huntington's disease. bioRxiv. 2023:2023.04.03.535397. doi: 10.1101/2023.04.03.535397.
- 49. Eleftheriou A, Ravotto L, Wyss MT, Warnock G, Siebert A, Zaiss M, et al. Simultaneous dynamic glucose-enhanced (DGE) MRI and fiber photometry measurements of glucose in the healthy mouse brain. NeuroImage. 2023;265:119762. doi: https://doi.org/10.1016/j.neuroimage.2022.119762.
- 50. Paech D, Schuenke P, Koehler C, Windschuh J, Mundiyanapurath S, Bickelhaupt S, et al. T1p-weighted Dynamic Glucose-enhanced MR Imaging in the Human Brain. Radiology. 2017;285(3):914-22. doi: 10.1148/radiol.2017162351. PubMed PMID: 28628422.
- 51. Kohonen T. The self-organizing map. Proceedings of the IEEE. 1990;78(9):1464-80. doi: 10.1109/5.58325.
- 52. Kim M, Eleftheriou A, Ravotto L, Weber B, Rivlin M, Navon G, et al. What do we know about dynamic glucose-enhanced (DGE) MRI and how close is it to the clinics? Horizon 2020 GLINT consortium report. Magnetic Resonance Materials in Physics, Biology and Medicine. 2022;35(1):87-104. doi: 10.1007/s10334-021-00994-1.
- 53. Gil-Mohapel J, Simpson JM, Ghilan M, Christie BR. Neurogenesis in Huntington's disease: Can studying adult neurogenesis lead to the development of new therapeutic strategies? Brain Research. 2011;1406:84-105. doi:
- https://doi.org/10.1016/j.brainres.2011.06.040.
- 54. Ahveninen LM, Stout JC, Georgiou-Karistianis N, Lorenzetti V, Glikmann-Johnston Y.

Reduced amygdala volumes are related to motor and cognitive signs in Huntington's disease: The IMAGE-HD study. NeuroImage: Clinical. 2018;18:881-7. doi: https://doi.org/10.1016/j.nicl.2018.03.027.

- 55. Shobe JL, Donzis EJ, Lee K, Chopra S, Masmanidis SC, Cepeda C, et al. Early impairment of thalamocortical circuit activity and coherence in a mouse model of Huntington's disease. Neurobiology of Disease. 2021;157:105447. doi: https://doi.org/10.1016/j.nbd.2021.105447.
- 56. Courtiol E, Wilson D. The olfactory thalamus: unanswered questions about the role of the mediodorsal thalamic nucleus in olfaction. Frontiers in Neural Circuits. 2015;9. doi: 10.3389/fncir.2015.00049.
- 57. Parent A, Mackey A, De Bellefeuille L. The subcortical afferents to caudate nucleus and putamen in primate: A fluorescence retrograde double labeling study. Neuroscience. 1983;10(4):1137-50. doi: 10.1016/0306-4522(83)90104-5.
- 58. Lebouc M, Richard Q, Garret M, Baufreton J. Striatal circuit development and its alterations in Huntington's disease. Neurobiology of Disease. 2020;145:105076. doi: <a href="https://doi.org/10.1016/j.nbd.2020.105076">https://doi.org/10.1016/j.nbd.2020.105076</a>.
- 59. Kaye J, Reisine T, Finkbeiner S. Huntington's disease mouse models: unraveling the pathology caused by CAG repeat expansion. Fac Rev. 2021;10:77. Epub 2021/11/09. doi: 10.12703/r/10-77. PubMed PMID: 34746930; PubMed Central PMCID: PMCPMC8546598.
- 60. Bailus BJ, Scheeler SM, Simons J, Sanchez MA, Tshilenge KT, Creus-Muncunill J, et al. Modulating FKBP5/FKBP51 and autophagy lowers HTT (huntingtin) levels. Autophagy. 2021;17(12):4119-40. Epub 2021/05/25. doi: 10.1080/15548627.2021.1904489. PubMed PMID: 34024231; PubMed Central PMCID: PMCPMC8726715.
- 61. Wang P, Yang J, Yin Z, Duan J, Zhang R, Sun J, et al. Amplitude of low-frequency fluctuation (ALFF) may be associated with cognitive impairment in schizophrenia: a correlation study. BMC Psychiatry. 2019;19(1):30. doi: 10.1186/s12888-018-1992-4.
- 62. Hallquist MN, Hwang K, Luna B. The nuisance of nuisance regression: Spectral misspecification in a common approach to resting-state fMRI preprocessing reintroduces noise and obscures functional connectivity. NeuroImage. 2013;82:208-25. doi: https://doi.org/10.1016/j.neuroimage.2013.05.116.

# 【評語】090016

# 1. Novelty and Significance:

This study introduces a novel approach to investigating Huntington's disease (HD) by utilizing Dynamic Glucose-Enhanced (DGE) MRI to examine glucose metabolism connectivity as a potential biomarker. The research is innovative in its application of advanced imaging techniques to explore metabolic disruptions in HD, a devastating neurodegenerative disorder. By employing two distinct mouse models, zQ175 KI and R6/2 KI, the study provides a comprehensive view of HD progression, from gradual to rapid disease development. This approach is significant as it offers a non-invasive method to potentially detect early metabolic changes in HD, which could be crucial for early diagnosis and intervention strategies. The use of self-organizing maps (SOM) to cluster DGE MRI signal curves further enhances the study's innovative aspect, revealing spatial and temporal connectivity variations that might be overlooked in conventional anatomical imaging.

# 2. Strength:

The study demonstrates several notable strengths. Firstly, it successfully identifies significant connectivity alterations in HD models, particularly in brain regions known to be associated with HD pathophysiology, such as the thalamus, caudate putamen, and dentate gyrus. This alignment with known HD pathology validates the approach and strengthens the potential of DGE MRI as a biomarker. Secondly, the use of two different mouse models allows for a more comprehensive understanding of HD progression, capturing both rapid (R6/2) and gradual (zQ175 KI) disease development. This dual-model approach enhances the study's relevance to various stages of HD. Additionally, the application of SOM clustering reveals distinct temporal patterns in glucose metabolism, providing insights into region-specific metabolic behaviors that may be crucial for understanding HD pathogenesis. The study's methodology offers a robust framework for future research into metabolic dysregulation in neurodegenerative diseases, potentially extending beyond HD.

# 3. Weakness:

While the clustering analysis reveals unique temporal patterns in glucose metabolism, the biological significance of these patterns remains unclear. Further research is needed

to establish a direct link between these metabolic behaviors and HD pathological mechanisms. Secondly, the study's potential for early HD diagnosis, while promising, requires additional validation. The variability in metabolic signals may impact their reliability as biomarkers, necessitating more extensive studies to confirm their accuracy in reflecting HD progression. To enhance the study's relevance, future work should include a more detailed introduction of the zQ175 KI and R6/2 KI mouse models, explaining their origins and the differences in disease severity, cognitive, behavioral, and motor symptoms between these strains. Additionally, the discussion should explore how the experimental results might explain these differences, providing deeper insights into HD pathogenesis. Lastly, methodological refinements to improve signal strength and address the complexity of SOM clustering could enhance the reliability of DGE MRI as a biomarker for HD.